SCHWEIZ. MINERAL. PETROGR. MITT. 81, 379–393, 2001

U–Pb SHRIMP geochronology of an amphibolitized eclogite and an orthogneiss from the Furgg zone (Western Alps) and implications for its geodynamic evolution

by *Anthi Liati*[1], *Dieter Gebauer*[1], *Nikolaus Froitzheim*[2] and *C. Mark Fanning*[3]

Abstract

In an attempt to clarify the nature and age of the Furgg zone in the Western Alps, an amphibolitized eclogite boudin within layered, impure dolomite and calcite marble in the area of Andolla (Antrona valley), and a leucocratic gneiss at Mattmark (Saas valley) were dated by ion microprobe (U–Pb SHRIMP-dating on zircon domains), assisted by cathodoluminescence (CL) imaging. Petrological and mineral chemical data from the amphibolitized eclogite indicate P_{min} of ca. 11 kbar for the HP stage and T of ca. 600 °C for the amphibolite-facies overprint. For the orthogneiss, metamorphic T were between 350° and 510 °C and P between ca. 9–11 kbar and ca. 7–8 kbar, as inferred from phengite core and rim compositions, respectively.

The uniform shape, size, CL-patterns and consistent magmatic ages of the zircons from the amphibolitized eclogite point to a gabbroic protolith rather than to basalt. The same is indicated also by the presence of magmatic chromite relics among the rock mineral constituents. Based on the CL-images, the zircons separated from this rock consist mainly of a large co-magmatic, oscillatory zoned domain surrounded by a thin (a few μm thick), U-poor metamorphic rim. Poor development of metamorphic rims is in line with the metamorphic grade of both rocks dated and the presence of relatively low amounts of fluids. Ion microprobe dating of the co-magmatic domains yielded a weighted mean age of 510 ± 5 Ma (95% c.l.), which is interpreted as the time of crystallization of the gabbroic protolith. An origin as Piemont-Ligurian (Middle/Upper Jurassic) or Valais (Upper Jurassic/Lower Cretaceous) oceanic crust is therefore excluded for the precursor of this amphibolitized eclogite of Andolla. An origin as a Mesozoic dyke intruding Triassic sediments is also excluded. SHRIMP analysis of the narrow, U-poor metamorphic rims show various degrees of inferred radiogenic Pb-loss and indicate that the rock was affected by Alpine metamorphism (after 87 ± 20 Ma, the youngest 'metamorphic age' obtained from the zircon rims). Moreover, a Triassic (229 ± 11 Ma) fluid/metamorphic event seems to be recorded in the metamorphic rims, as is the case also in many other areas of the Alps (e.g. Dora Maira massif, Ivrea zone, Sesia zone).

Zircons separated from the orthogneiss of Mattmark indicate by their typology a magmatic precursor (a granitoid or an acid volcanic rock). They consist mainly of large co-magmatic, oscillatory domains, surrounded by narrow metamorphic rims. SHRIMP-dating of the co-magmatic domains yielded a weighted mean age of 272 ± 4 Ma (95% c.l.), which is interpreted as the time of crystallization of the magmatic protolith. The metamorphic age is not resolvable, due to the very limited thickness and U-poor composition of the metamorphic rims. The latter show loss of radiogenic Pb implying an Alpine metamorphic imprint.

Based on these SHRIMP results and considering previously reported lithostratigraphic/structural arguments, the Furgg zone – at least its northern part along the northern rim of the Monte Rosa nappe – is interpreted as a tectonic mélange of strongly heterogeneous rock constituents including Variscan/pre-Variscan basement, as well as post-Variscan rocks.

Keywords: Furgg zone, Monte Rosa, Western Alps, SHRIMP-dating, U–Pb geochronology, zircon.

[1] Institut für Isotopengeologie und Mineralische Rohstoffe, ETH-Zentrum, Sonneggstrasse 5, CH-8092 Zürich, Switzerland. <liati@erdw.ethz.ch>, <gebauer@erdw.ethz.ch>

[2] Geologisches Institut, Universität Bonn, Nussallee 8, 53115 Bonn, Germany. <niko.froitzheim@uni-bonn.de>

[3] Research School of Earth Sciences, Australian National University, Mills Road 0200 ACT Canberra, Australia. <Prise.Fanning@anu.edu.au>

1. Introduction

The Furgg zone (BEARTH, 1952; WETZEL, 1972) is an intensely deformed tectonic element of the Western Alps, separating the Monte-Rosa nappe from surrounding units (Fig. 1). The characteristic lithology of the Furgg zone is represented by overprinted eclogite boudins within a matrix of schists, leucocratic gneisses, quartzites and metacarbonates. The exact location and extent of the Furgg zone, as well as the nature, origin, and age of both the boudins and matrix rocks are a matter of controversy (for a review see DAL PIAZ, 2001). Several serpentinite and amphibolite layers are intercalated within the boudin-bearing series. These ophiolites are similar to and, in one case, directly connected with the Mesozoic Antrona ophiolites. The ophiolites are either included in the Furgg zone (MILNES et al., 1981; FROITZHEIM, 2001) or considered as belonging to separate tectonic units (Zermatt-Saas, Antrona) isoclinally folded together with the Furgg zone (JABOYEDOFF et al., 1996). The Furgg zone has been interpreted either as a deformed sedimentary cover series, Late Carboniferous–Permian to Middle Jurassic (JABOYEDOFF et al., 1996) or even to Cretaceous in age (STECK et al., 1999), or as an ophiolite-bearing, tectonic mélange (MILNES et al., 1981; KRAMER, 2000; FROITZHEIM, 2001). A very similar series occurring on the southern side of the Monte Rosa massif, between the Monte Rosa orthogneiss and the overlying Zermatt-Saas zone, but at a deeper level within the Monte Rosa nappe as well, was interpreted as heterogeneous Hercynian basement (DAL PIAZ, 1966). This series, however, is devoid of ophiolitic intercalations.

The nature of the Furgg zone has important implications for the paleogeographic restoration and geodynamic evolution of the Alps. Based on the mélange hypothesis and on structural arguments, MILNES et al. (1981) and FROITZHEIM (2001) assumed that the Monte Rosa nappe is a structurally deeper unit, derived from north of the Briançonnais-Bernhard nappe and that the two were separated by an oceanic basin. This view is in contrast to the classical interpretation, which relo-

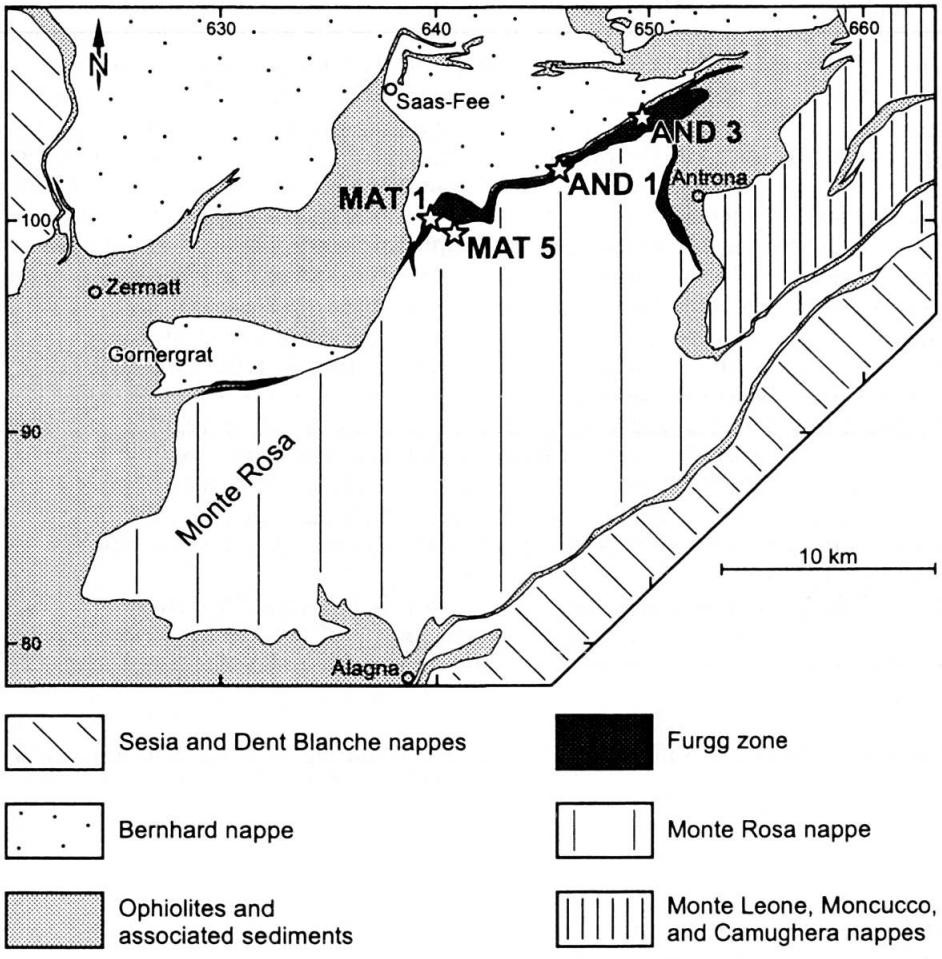

Fig. 1 Geological outline of the Furgg zone and surrounding units with sample locations shown by stars (map from STECK et al., 1999).

cates the Monte Rosa nappe south of the Bernhard nappe (e.g., ESCHER et al., 1997). In an attempt to clarify these issues by means of geochronology, we applied the U–Pb ion microprobe dating technique (SHRIMP) on zircon domains from an amphibolitized eclogite boudin within layered, impure dolomite and calcite marble in the area of Andolla, as well as from a leucocratic gneiss in the Mattmark area (Fig. 1). Cathodoluminescence (CL) images of all zircons analyzed have been used to distinguish between magmatic and metamorphic zircon domains, and to avoid the analysis of areas that would yield a mixture of ages.

2. Geological setting and field relations of the dated rocks

The amphibolitized eclogite dated (sample AND1; Fig. 1) is from an outcrop on the southwestern rim of Ghiacciaio del Bottarello in the Andolla area, upper Valle Loranco (Swiss coordinates 646.112, 102.575). It represents a metabasite boudin, several metres thick, embedded in layered, impure dolomite and calcite marble. The metasedimentary country rock of the dated metabasite boudin may be interpreted as Triassic for its strong lithological similarity with dated rocks of that age (KELLER, 2000; KELLER and SCHMID, 2001). Similar marbles at the contact between the Bernhard nappe and the Zermatt-Saas ophiolites (2 km southwest of locality "MAT1" in Fig. 1) are considered to be Triassic on the basis of the presence of the crinoid *Encrinus liliiformis* (GÜLLER, 1947). On the Monte Rosa map of STECK et al. (1999), the metasediments surrounding the dated amphibolitized eclogite boudin belong to the lithology "marbres et flysch à blocs, Trias–Crétacé" which is equivalent to the "middle" and "upper" Furgg zone of JABOYEDOFF et al. (1996). In contrast, KELLER (2000) and KELLER and SCHMID (2001) do not include these metasediments in the Furgg zone, but rather consider them as remnants of the sedimentary cover of the Monte Rosa nappe, separated from the Furgg zone, which, according to these authors, is exposed about 300 m farther northeast on the other side of the Ghiacciaio del Bottarello. In any case, both interpretations imply a Mesozoic or younger age for the protolith of the eclogite. The leucocratic gneiss (MAT1) was sampled northwest of Mattmark dam in the upper Saas valley along a stream near the tongue of the Allalingletscher (Swiss coordinates 639.850, 100.225). In this area the Furgg zone is devoid of carbonate rocks and consists of schists and leucocratic gneisses with metabasite boudins. Some of the schists contain deformed quartz pebbles and are interpreted as Permian to Lower Triassic metaconglomerates (e.g. Fig. 3B in FROITZHEIM, 2001). No such sedimentary structures were observed, however, within the layer from which sample MAT1 was taken. On the Monte Rosa map (STECK et al., 1999) the locality again belongs to the lithology "marbres et flysch à blocs, Trias–Crétacé". In addition to these two samples, we collected also a quartz vein (sample AND3) located between an eclogite boudin and its country rock (mica schist) at Alpe Campolamana in Valle Loranco (Furgg zone, Swiss coordinates 649.475, 104.725; Fig. 1), as well as a kyanite-talc schist (sample MAT5) within a shear zone of the Monte Rosa basement, 120 m south of its northern boundary against the Furgg zone (eastern side of the Mattmark Lake; Swiss coordinates 640.700, 99.700; Fig. 1). According to WEBER (2001) the locality of this sample is at the contact between deformed Monte Rosa granite and pre-granitic paragneiss. First results from these samples are discussed in this paper for comparison (Section 8) and analytical data are listed in table 1 (AND3: analysis 8; MAT5: analyses 24, 25).

3. Petrology and mineral chemistry of the dated rocks

The chemical composition of the main mineral constituents of the rocks dated was identified by electron microprobe. The electron microprobe analyses were carried out with a Cameca SX51 (at 15 kV, 20 nA) at the Institute of Mineralogy, University of Heidelberg. Here, the most important data on the mineral composition are given. Complete microprobe analyses of minerals are available by the authors upon request.

3.1. AMPHIBOLITIZED ECLOGITE

The common mineral assemblage of this rock is: garnet-omphacite-glaucophane-sodic-augite-albite-paragonite-Ca-Na-amphibole (barroisite)-Ca-amphibole-clinozoisite/epidote-quartz-calcite-rutile.

The rock shows partial post-HP overprint marked mainly by the extensive development of very fine sodic augite-albite symplectites at the expense of primary omphacite. Replacement of symplectitic clinopyroxene and garnet by Ca-amphibole + plagioclase and of Ca-Na-amphibole by Ca-amphibole is also observed.

Garnet is slightly zoned showing an increase in pyrope (Py) and grossular (Gr) and decrease in

almandine (Alm) and spessartine (Sp) contents from core to rim. The composition of the core is: $Alm_{65-70}Gr_{18.5-14.5}Py_{13}Sp_{3.5-2.5}$ and that of the rim: $Alm_{60-62}Gr_{21-17.5}Py_{17.5-19}Sp_{1.5-2.5}$.

Omphacite relics are partly preserved in the matrix. However, these may be already breakdown products of primary Jd-richer omphacites. The maximum jadeite content of the analyzed omphacite relics is 36 mol%.

Different types of *amphibole* are distinguished both on textural grounds and by chemical composition. Analyzed amphiboles were identified as Na-amphiboles (glaucophane), Na-Ca-amphiboles (barroisite) and Ca-amphiboles (e.g. Ca-poor actinolite, Ca-poor magnesio-hornblende, Al-rich, Si-poor ferropargasite). The prevailing amphibole types in the matrix are Na-Ca- and Ca-amphibole. Na-amphibole (glaucophane) is preserved as a primary HP relic surrounded by very fine grained symplectites of Na-rich plagioclase + green amphibole. It is worth mentioning that the chemical composition of the glaucophane is quite exceptional in that it is very rich in Cr (ca. 7.3 wt% Cr_2O_3) and has very little iron, thus approaching the pure Mg-member. Incorporation of Cr in glaucophane is probably related to destabilization of chromite, which still occurs as relic (magmatic) grains in the immediate vicinity. The presence of chromite favors the view that the precursor of the amphibolitized eclogite was a gabbro. As discussed later, this view is further supported by the shape, size and CL-pattern of the zircons (see section 6).

PT conditions of metamorphism and correlation with zircon geochronology: Garnet and omphacite are no longer in direct contact due to extensive symplectization of initial omphacite to diopside + Na-rich plagioclase. Hence, the cpx-garnet geothermometer cannot be applied to derive peak metamorphic conditions during the HP stage. Nevertheless, the maximum jadeite content (Jd_{36}) analyzed in relic omphacite (but possibly not representing the primary omphacite composition) implies minimum pressures of ca. 11 kbar, for assumed temperatures of ca. 550 °C (based on GASPARIK and LINDSLEY, 1981). The grt-amph geothermometer (GRAHAM and POWELL, 1984) between garnet rim and the neighboring green amphibole yields T around 600 °C for the amphibolite-facies overprint.

Based on the results of the petrological study of the amphibolitized eclogite, we expect that zircon in this rock should not have been much – if at all – affected (recrystallized) during metamorphism. This is because under temperatures of metamorphism up to 600–650 °C, recrystallization of zircon is very limited, unless abundant fluids occur (e.g. GEBAUER et al., 1989; GEBAUER, 1996; RUBATTO and GEBAUER, 2000). The apparent presence of relatively low amounts of fluids in this rock (indicated by the preservation of omphacite) probably contributed to poor development of metamorphic domains of the zircon crystals. CL-images of the zircons show indeed very narrow recrystallization rims (see below, section 6). It is not clear at which stage of metamorphism (peak pressure or overprint) the zircon rims formed. Characteristic mineral inclusions were not found within the metamorphic rims.

3.2. LEUCOCRATIC GNEISS (ORTHOGNEISS)

The common mineral assemblage of this rock is: albite-quartz-K-white mica-clinozoisite/epidote-garnet-titanite.

K-white mica has elevated Si contents and shows some zoning (core: ca. 3.40 Si atoms p.f.u.; rim: ca. 3.30 Si atoms p.f.u.), which indicates re-equilibration at lower pressures during metamorphic overprint.

Garnet is rich in Mn and shows chemical zoning (core: $Alm_{33-34}Gr_{45-46}Py_{0.5}Sp_{20}$, rim: $Alm_{39-40}Gr_{38-39}Py_{0.7}Sp_{20-22}$).

Titanite is rich in Al (Al_2O_3: ca. 6.9 wt%).

PT conditions of metamorphism and correlation with zircon geochronology: Grt-phengite thermometry (KROGH and RAHEIM, 1978; GREEN and HELLMAN, 1982; HYNES and FOREST, 1988) yields temperatures ranging between 350–510 °C. Based on the Si content of phengite (MASSONNE and SCHREYER, 1987), minimum pressures of 9–11 kbar (for core compositions) and 7–8 kbar (for rim compositions) result for this temperature range (assuming $\alpha_{H_2O} = 1$). Similar to the amphibolitized eclogite of Andolla, zircon in the orthogneiss is not expected to show large – if any – recrystallization rims, due to the relatively low temperatures of metamorphism (see above). This argument is in agreement with the CL-images of the zircons from this rock (see below, section 6).

4. Dating technique and cathodoluminescence imaging

The U–Pb ion microprobe data presented in this paper were obtained mainly using SHRIMP II, at the Australian National University in Canberra. Four analyses from the Andolla eclogite were carried out with SHRIMP II at the Geological Survey of Canada, in Ottawa (Tab. 1). For the magmatic zircon domains we used a spot size of ca. 20 μm whereas for most metamorphic domains we

Tab. 1 U, Th, Pb SHRIMP data for zircons from the amphibolitized eclogite of Andolla (AND1), the quartz vein around an eclogite boudin, Alpe Campolamana (AND3), the orthogneiss at Mattmark (MAT1) and the kyanite-talc schist, Monte Rosa basement, Mattmark (MAT5).

Sample	U (ppm)	Th (ppm)	Th/U	rad. Pb (ppm)	f^{206}Pb (%)	^{207}Pb/^{206}Pb (1σ) (uncorrected)	^{238}U/^{206}Pb (1σ) (uncorrected)	^{206}Pb/^{238}U (1σ) (radiogenic)	age (Ma) ^{206}Pb/^{238}U (1σ)
Amphibolitized eclogite, Andolla (AND1) and quartz vein around eclogite boudin, Alpe Campolamana (AND3)									
co-magmatic, oscillatory zircon domains									
1. AND1-3A.2	1222	1118	0.91	166	0.00	0.0571 ± 0.0004	12.14 ± 0.14	0.0824 ± 0.0010	510.4 ± 5.8
2. AND1-5.1	1004	2737	2.73	198	0.01	0.0581 ± 0.0003	12.03 ± 0.13	0.0831 ± 0.0009	514.5 ± 5.5
3. AND1-7.1	924	763	0.83	124	0.01	0.0575 ± 0.0004	12.10 ± 0.14	0.0827 ± 0.0010	512.0 ± 5.6
4. AND1-11.1	983	880	0.89	134	0.00	0.0570 ± 0.0006	12.10 ± 0.16	0.0827 ± 0.0011	512.1 ± 6.6
5. AND1-13.1	1560	1703	1.09	221	0.00	0.0571 ± 0.0004	12.09 ± 0.13	0.0827 ± 0.0009	512.3 ± 5.3
6. AND1-9.1	973	805	0.83	128	0.00	0.0576 ± 0.0003	12.33 ± 0.13	0.0811 ± 0.0009	502.7 ± 5.2
7. AND1-22.2	*1773*	*4250*	*2.40*	*321*	*0.00*	*0.0573 ± 0.0003*	*12.56 ± 0.15*	*0.0796 ± 0.0009*	*494.0 ± 5.5*
8. AND3-10.2	*711*	*616*	*0.87*	*93*	*0.00*	*0.0579 ± 0.0003*	*12.48 ± 0.14*	*0.0801 ± 0.0009*	*496.4 ± 5.4*
metamorphic rims							***Weighted mean: 510 ± 5Ma (95% c.l.)***		
9. AND1-3A.1	2	0	0.11	0	0.00	0.4208 ± 0.0842	38.70 ± 4.07	0.0137 ± 0.0031	87.4 ± 19.8
10. AND1-5.2	59	91	1.53	7	0.12	0.0629 ± 0.0016	16.09 ± 0.34	0.0614 ± 0.0013	384.4 ± 7.9
11. AND1-6.1	1	1	1.11	0	4.88	0.6123 ± 0.0644	10.68 ± 2.06	0.0274 ± 0.0092	174.0 ± 58.2
12. AND1-8.A•	91	36	0.40	7	0.00	0.2152 ± 0.0422	20.49 ± 0.95	0.0394 ± 0.0019	224.0 ± 11.5
13. AND1-9.2	11	7	0.58	1	0.50	0.0823 ± 0.0052	16.61 ± 0.68	0.0581 ± 0.0024	364.0 ± 14.6
14. AND1-9.3	245	231	0.94	30	0.03	0.0605 ± 0.0008	13.35 ± 0.19	0.0745 ± 0.0010	463.3 ± 6.3
15. AND1-9.A•	65	12	0.19	1	0.31	0.2614 ± 0.0208	22.33 ± 1.00	0.0336 ± 0.0019	212.9 ± 11.7
16. AND1-13.A•	214	211	1.02	19	0.02	0.0741 ± 0.0017	13.14 ± 0.37	0.0745 ± 0.0021	463.1 ± 12.5
17. AND1-22.1	15	9	0.63	1	0.65	0.0962 ± 0.0112	24.54 ± 1.82	0.0385 ± 0.0029	243.2 ± 18.1
18. AND1-22.1A	44	50	1.14	3	0.15	0.0710 ± 0.0026	26.06 ± 0.93	0.0374 ± 0.0013	236.8 ± 8.3
19. AND1-22.A•	115	260	1.029	14	<0.01	0.1558 ± 0.0092	39.37 ± 1.92	0.0222 ± 0.0011	141.5 ± 7.1
Orthogneiss Mattmark (MAT1) and talc-kyanite-schist, Monte Rosa basement (MAT5)									
co-magmatic, oscillatory zircon domains									
20. MAT1-1.1	421	128	0.30	26	0.01	0.0521 ± 0.0008	23.21 ± 0.29	0.0431 ± 0.0005	271.8 ± 3.4
21. MAT1-1.3	450	145	0.32	20	0.01	0.0533 ± 0.0009	23.13 ± 0.30	0.0432 ± 0.0006	272.3 ± 3.5
22. MAT1-3.1	246	11	0.04	14	0.01	0.0544 ± 0.0008	23.43 ± 0.32	0.0425 ± 0.0006	268.5 ± 3.6
23. MAT1-4.1	1211	351	0.29	74	0.00	0.0523 ± 0.0005	23.01 ± 0.26	0.0434 ± 0.0005	274.0 ± 3.0
24. MAT5-27.2	*2001*	*11*	*0.005*	*82*	*0.01*	*0.0520 ± 0.0005*	*22.99 ± 0.25*	*0.0435 ± 0.0005*	*274.4 ± 3.0*
25. MAT5-24.2	*2217*	*80*	*0.036*	*93*	*0*	*0.0522 ± 0.0004*	*22.83 ± 0.26*	*0.0438 ± 0.0005*	*276.2 ± 3.1*
metamorphic rim							***Weighted mean: 272 ± 4 Ma (95% c.l.)***		
23. MAT1-1.2	160	50	0.31	9	0.09	0.0641 ± 0.0014	25.29 ± 0.41	0.0389 ± 0.0006	246.0 ± 3.9
inherited zircon									
24. MAT1-2.2	1103	222	0.20	113	0.00	0.0625 ± 0.0008	9.84 ± 0.15	0.1014 ± 0.0016	622.4 ± 9.3
25. MAT1-2.1	565	26	0.05	41	0.01	0.0563 ± 0.0011	17.81 ± 0.21	0.0560 ± 0.0007	351.0 ± 4.0

f^{206}Pb% denotes the percentage of ^{206}Pb that is common Pb.
Analyses with a black spot (•) were obtained at the Geological Survey of Canada, Ottawa. All others at ANU, Canberra.
Analyses in *italics* (Nr. 7, 8 and 24, 25) are not considered in the weighted mean age calculation (see text).

chose a spot size of ca. 10 µm, due to the narrow rim domains. For data collection, seven scans through the critical mass range were made. Further details on the SHRIMP technique are to be found in WILLIAMS (1998).

Cathodoluminescence (CL) images of the zircon crystals dated were obtained both before SHRIMP-dating, for distinguishing different zircon domains, as well as after SHRIMP-dating to confirm the exact location of the spots. CL-images provided useful information also on the formation history of the different zircon domains since they reveal internal patterns characteristic of the formation conditions. In general, strong CL means high amounts of minor and trace elements, weak CL means low amounts of minor and trace elements, including U. To facilitate interpreting the CL-pictures, we note that the darker the zircon (weaker CL-emission), the higher the U content. This is a visual way to estimate the relative U contents via CL. Additional very important information provided via CL-images regards the fissures present in the zircon crystals. In the zircons of the Andolla eclogite in particular, but also in those of the Mattmark gneiss, cracks are observed only in the CL-images while in secondary electron (SE) images they are not visible, because they have healed. Narrow, CL-bright zones are observed on either side of these cracks (e.g. Fig. 2A, or 3B or 4). It seems that fluids circulating along the cracks led to recrystallization of zircon and Pb-loss, thus resulting in younger ages (see below).

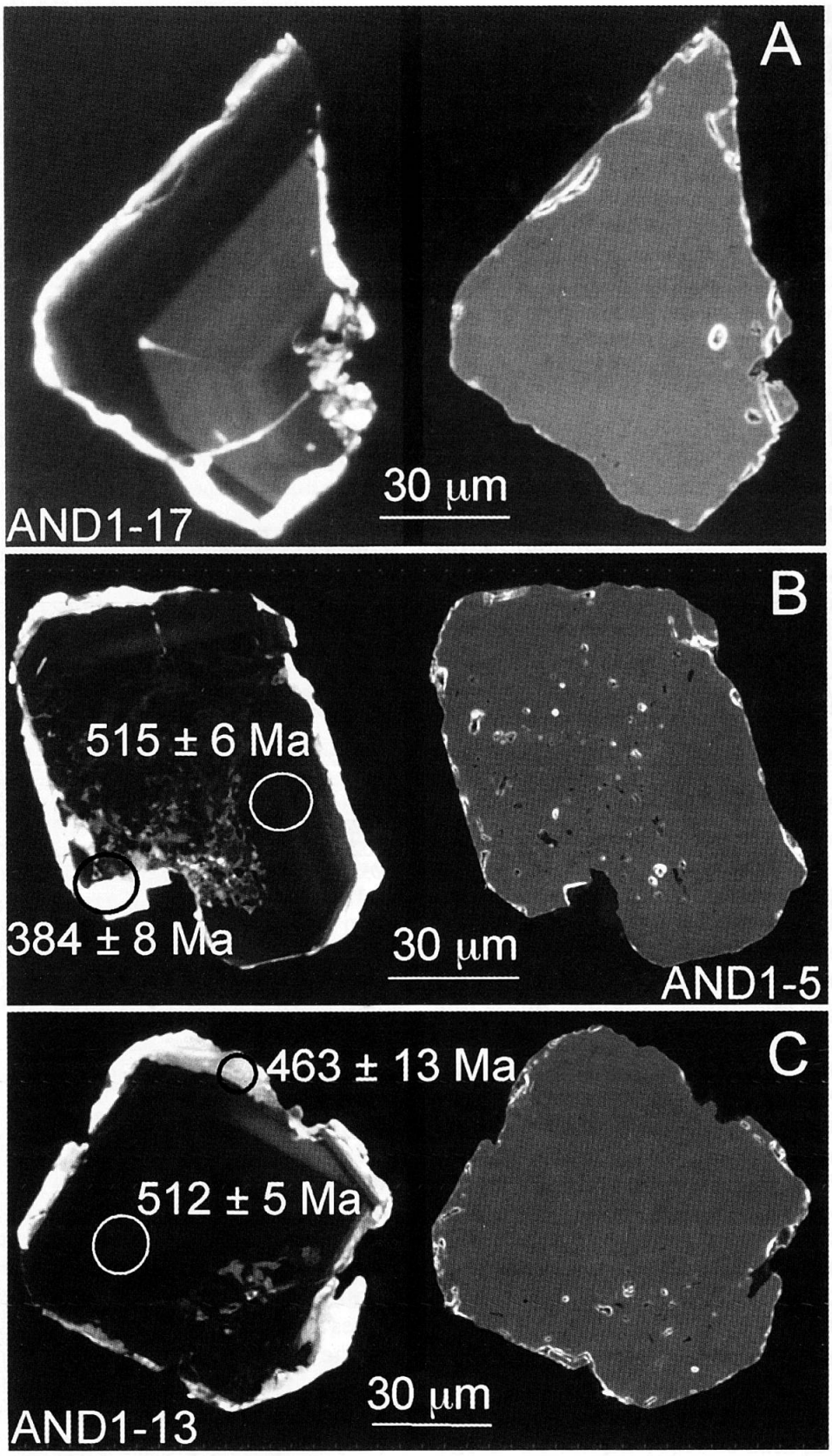

Fig. 2 Cathodoluminescence (CL) pictures (left) and secondary electron (SE) pictures (right) of co-magmatic zircon crystals from the amphibolitized eclogite of Andolla. As shown in CL-pictures, zircons consist essentially of a magmatic part (dark in CL) surrounded by a very narrow metamorphic rim (bright in CL). In (A) broad oscillatory zoning is evident. In the lower part of the zircon in (A) a crack (bright in CL) crosscuts the crystal; this is not visible in the SE-picture. The same is true for C (lower parts of the crystal, bright in CL). Most inclusions in zircons (especially visible in (B) are melt inclusions. Note also that the spot analyses of metamorphic (bright) rims lie partly in the co-magmatic part and therefore yield mixed ages. This was inevitable, due to the very thin rims.

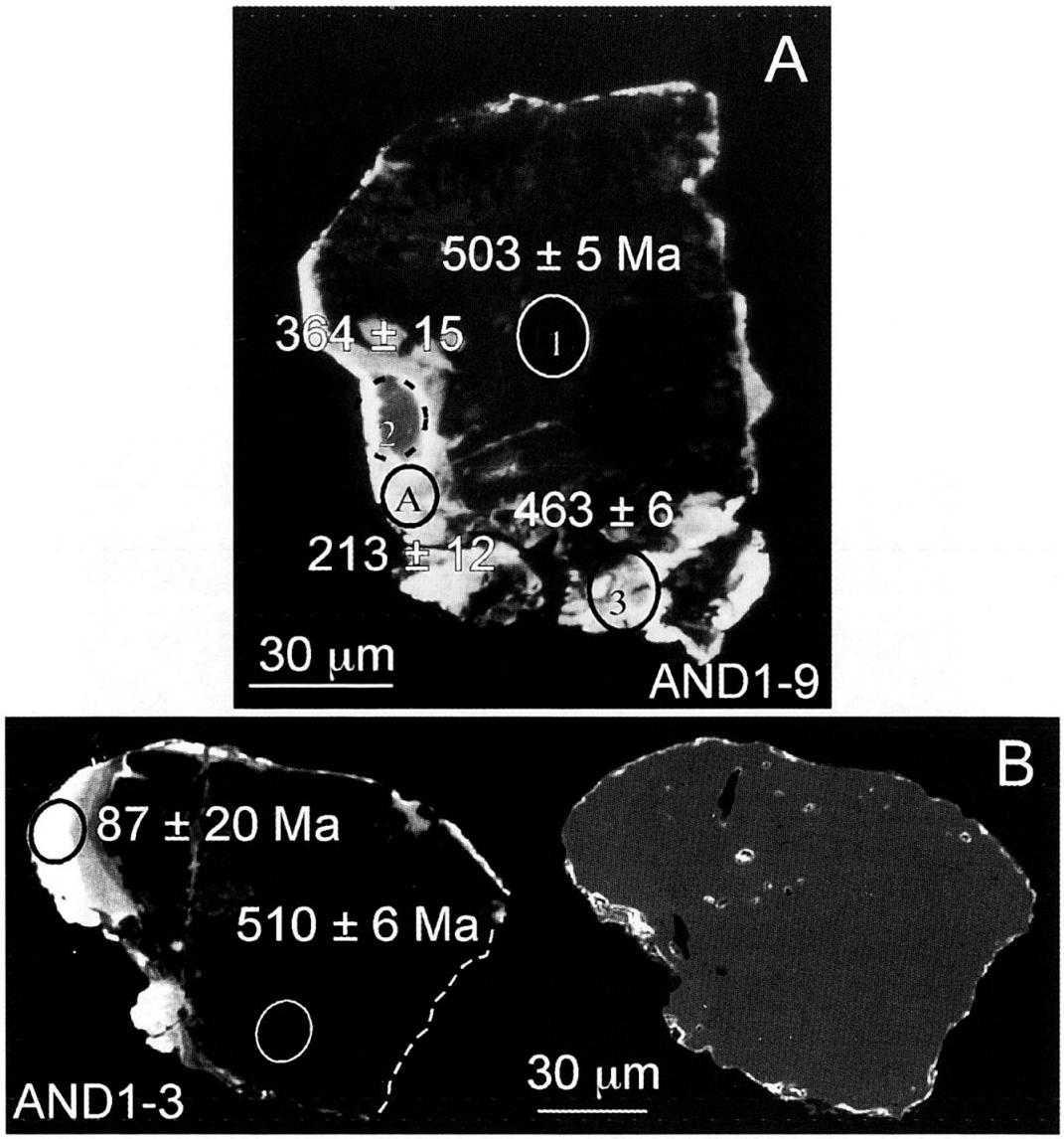

Fig. 3 Cathodoluminescence (CL) pictures (A and left side in B) and secondary electron (SE) pictures (right side in B) of co-magmatic zircon crystals from the amphibolitized eclogite of Andolla. In (A) note that the pit generated during SHRIMP analysis (Nr. 2) shows weak CL (dark appearance), which is interpreted to be due to the presence of an underlying magmatic core (see text). In (B) note the two distinct metamorphic rims (inner darker and outer lighter in CL) formed by recrystallization probably during different stages of metamorphism or during different metamorphic episodes (see also text).

The CL-pictures of zircon crystals were produced at the ETH in Zurich from a split screen on a CamScan CS 4 scanning electron microscope (SEM) operating at 13 kV (see GEBAUER 1996 for detailed technical description). Secondary electron (SE) pictures were produced simultaneously with the CL-pictures using a different detector.

5. Data evaluation

For the calculation of the $^{238}U/^{206}Pb$ ratios and ages, the data were corrected for common Pb using the ^{207}Pb correction method. The data are graphically presented on Tera-Wasserburg (TW) diagrams, where total $^{207}Pb/^{206}Pb$ vs. the calibrated total $^{238}U/^{206}Pb$ is plotted.

The amount of common Pb was calculated using the isotope composition of common Pb obtained from the model of CUMMING and RICHARDS (1975). This model was chosen because the analyzed spots plot in the Tera-Wasserburg diagram along a mixing line intersecting the y-axis at the isotopic composition $^{207}Pb/^{206}Pb = 0.870$ (for the case of Andolla amphibolitized eclogite) and 0.852 (for the case of the Mattmark gneiss). These values correspond to the $^{207}Pb/^{206}Pb$ ratio at the time of formation of the corresponding zircon do-

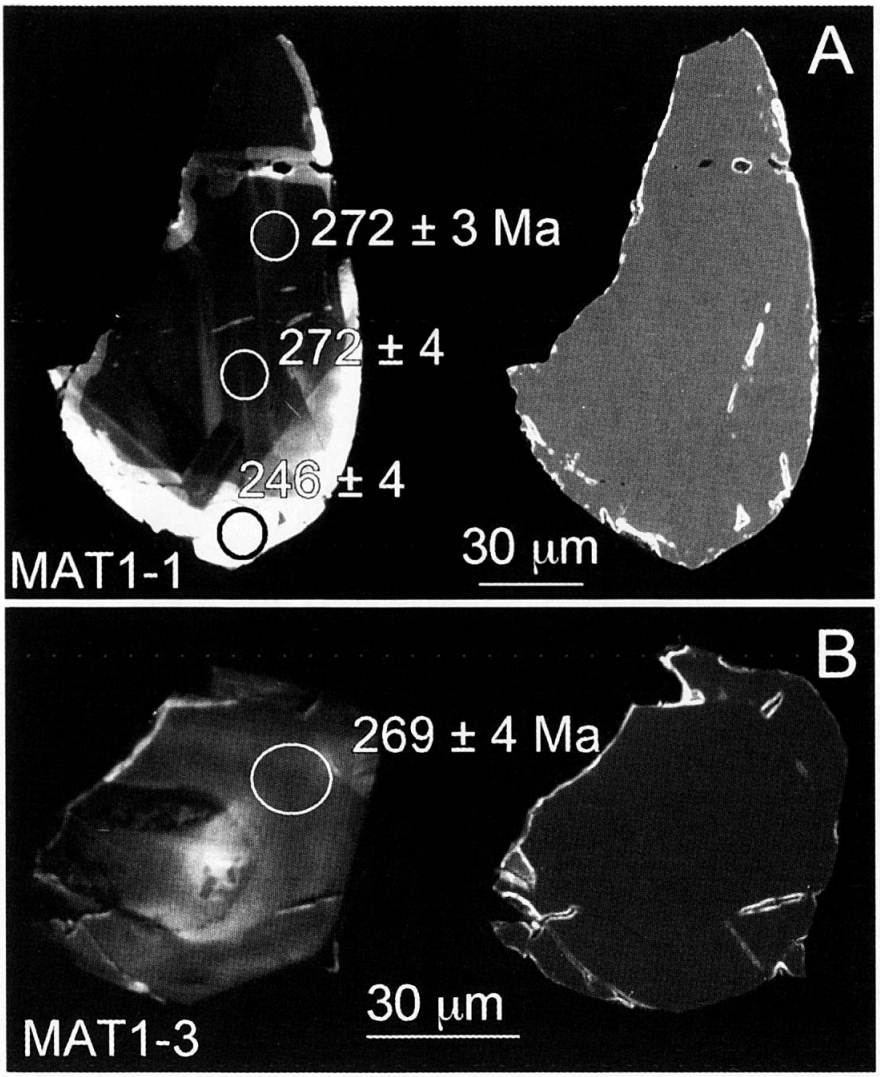

Fig. 4 Cathodoluminescence (CL) pictures (left) and secondary electron (SE) pictures (right) of co-magmatic zircon crystals from the orthogneiss of Mattmark. The zircons exhibit mainly a large co-magmatic core (dark in CL) with oscillatory zoning. A thin rim (bright in CL) forming as a result of metamorphism is shown in (A). Bright CL is shown also on either side of a crack in upper part of (A) (not visible in SE; see text). In zircon crystal (B) no metamorphic rim developed, as is evident in the CL-pattern.

main. The error bars of the individual data points plotted are 2σ errors.

The U/Pb ratios were calibrated relative to the AS3 reference zircon (PACES and MILLER, 1993). U and Th concentrations as listed in table 1, however, were calculated relative to SL13.

For single spot analysis 1σ errors are given for the age data in table 1. The ages were calculated as weighted mean ages, since they are more representative of the analytically best measurements. These weighted mean ages are given at the 95% confidence level (c.l.), taking into consideration the 1σ analytical error shown in table 1.

6. CL characteristics, morphology and interpretation of the formation history of the zircon crystals dated

6.1. AMPHIBOLITIZED ECLOGITE

Zircons separated from the amphibolitized eclogite of Andolla still show the originally euhedral (magmatic) shapes although they are partly fragmented and their outer surfaces may show some irregularities, due to metamorphism. Grains are relatively equidimensional and ca. 100–140 μm in size. CL-images of the sectioned grains reveal that they consist mainly of a large magmatic, oscillatory zoned part with relatively wide spacing of the oscillating domains, typical for zircons formed in a

gabbroic melt (e.g. RUBATTO and GEBAUER, 2000), surrounded by a narrow, light in CL, metamorphic rim (Figs 2, 3). In some cases, the magmatic domain contains melt inclusions. The large size of the zircons in combination with the oscillatory CL-pattern of the magmatic domains indicates that they crystallized from a slowly cooling melt and therefore point to a gabbroic protolith of the amphibolitized eclogites. The metamorphic domains are developed at the rim of the zircon crystals. They are very bright in CL and have low U and Th contents. Their Th/U ratio is relatively high for metamorphic (or recrystallized) zircons, but is still lower than in the co-magmatic domain of the same zircon crystal (Tab. 1). The metamorphic rims are very narrow, usually a few μm wide and are interpreted to have resulted from recrystallization during metamorphism. Recrystallization started from the rims and proceeded also along cracks across the grains. This is evident in some zircons, which show bright CL along cracks propagating inside the magmatic domain (e.g. Fig. 2A). These cracks are only visible in CL, whereas in the SE-pictures they are not detectable. It seems that they were healed at later stages of metamorphism. This is a very important observation for the interpretation of the SHRIMP data (see below). CL-imaging is therefore a very useful tool also for detecting healed cracks, which otherwise would be ignored and would possibly lead to not only incorrect geochronological but also petrological interpretations (cf. GEBAUER et al., 1997). In some cases, metamorphic rims of the dated zircons show two domains: a slightly CL-darker inner rim domain and a very bright outermost one (e.g. Fig. 3B). These two distinct rim domains may reflect different amounts of Pb-loss caused by metamorphic recrystallization of the original magmatic zircons during different stages of metamorphism (e.g. the inner rim during HP metamorphism and the outer one during the amphibolite-facies overprint) or during different metamorphic episodes.

It is worth mentioning that the morphology and CL-pattern of the zircons within the quartz vein at Alpe Campolamana (sample AND3), which are inherited in the quartz vein from the neighboring amphibolitized eclogite boudin, are identical to those of the amphibolitized eclogite AND1 from Andolla.

6.2. LEUCOCRATIC GNEISS

Zircons separated from the gneiss are relatively large (100–250 μm long, 60–120 μm wide). The majority of the grains are euhedral but there are also zircons with relatively rounded outlines, possibly due to magmatic resorption. CL-images reveal that the zircon crystals consist mainly of a magmatic core with weak luminescence (dark appearance) and oscillatory zonation, surrounded by a thin (a few μm thick), strongly luminescing (bright) rim. Locally, the rim gets a little wider, up to ca. 25 μm (e.g. Fig. 4A), but there are cases where a metamorphic rim is hardly visible (Fig. 4B). Bright CL is also observed in narrow zones on either side of cracks (e.g. Fig. 4A). These CL patterns and crystal form characteristics indicate a magmatic protolith (either a granitoid or a rhyolite) and therefore suggest that the rock is an orthogneiss.

Regarding the kyanite-talc schist within a shear zone of the Monte Rosa basement (sample MAT5), zircon crystals show oscillatory zoned, probably co-magmatic domains with darker (more U-rich) outermost parts. A milky pattern, partly obliterating the oscillatory zoning, is shown by some crystals, possibly as a result of interaction with fluids.

7. SHRIMP results and interpretation

The ion microprobe data for the analyzed zircons are given in table 1 and plotted on Tera-Wasserburg diagrams (Figs 5 and 6). Weighted mean ages and errors (given at the 95% confidence level) are given both on the diagrams as well as in table 1.

7.1. AMPHIBOLITIZED ECLOGITE

Eighteen data points were obtained from 10 different grains of zircon from the amphibolitized eclogite of Andolla. Seven of them are from the co-magmatic domains and eleven from the metamorphic rims. Data from the co-magmatic domains are plotted in figure 5A. This figure shows six of the analyzed spots plotting along a mixing line with common Pb and $^{238}U/^{206}Pb$ as end members, while the other analysis (7 of table 1) shows slight radiogenic Pb-loss. Careful inspection of the CL-picture of this zircon grain, obtained after SHRIMP work, shows that the analyzed spot partly touches the metamorphic rim. As a result, a slightly younger 'age' is obtained from this spot, which we omit in the mean age calculation. The weighted mean age of the six spots that are located well within the co-magmatic domains is 510 ± 5 Ma (95% c.l.). This age is interpreted as the crystallization time of the amphibolitized eclogite protolith.

Ten spots were analyzed from CL-bright metamorphic domains. The thin metamorphic rims,

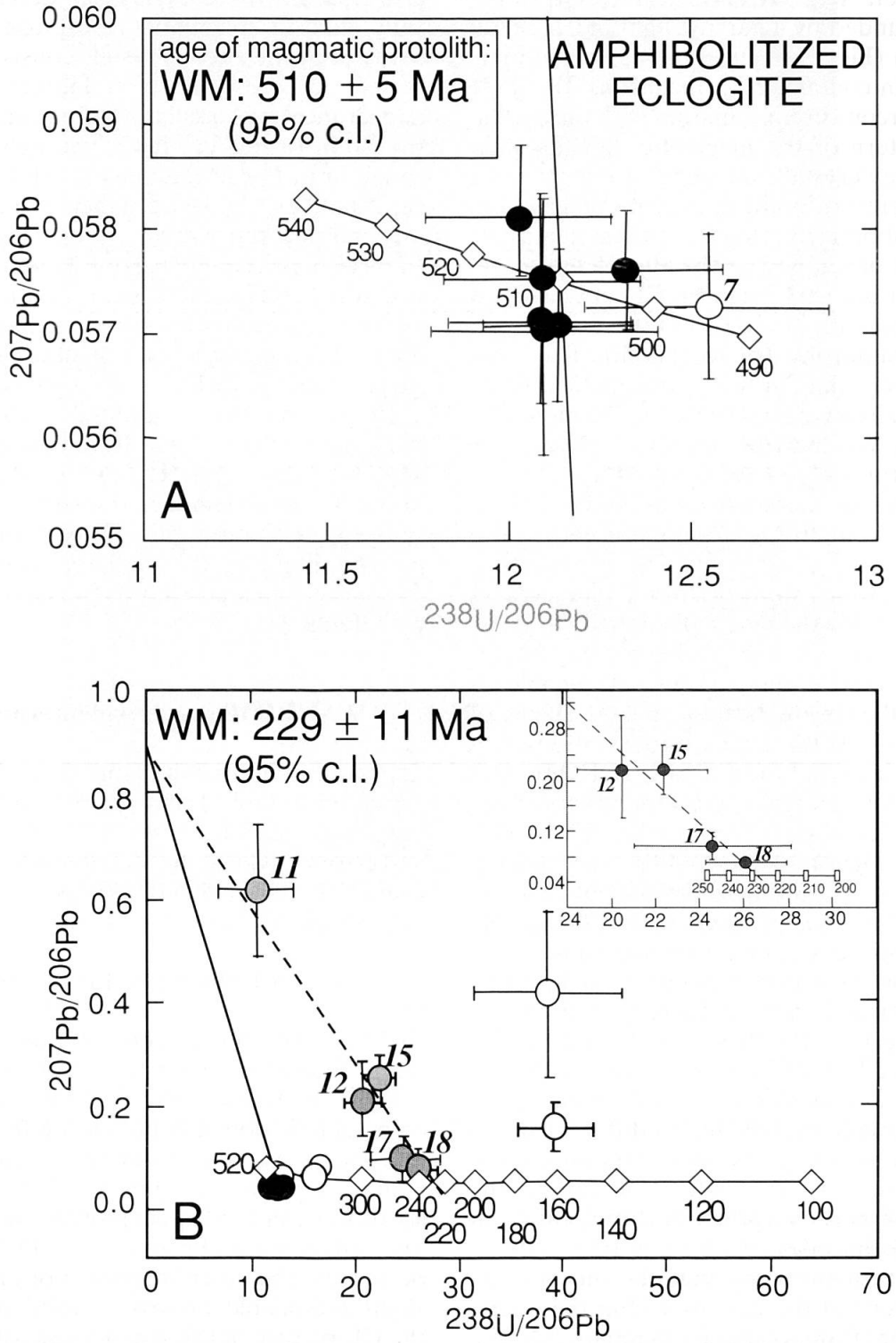

Fig. 5 Tera-Wasserburg diagrams with data of zircons from the amphibolitized eclogite of Andolla. In (A) six analyses from the co-magmatic, oscillatory zoned zircon domains plot along a mixing line with common Pb (composition from the model of CUMMING and RICHARDS, 1975) and $^{238}U/^{206}Pb$ as end members, intersecting the concordia at 510 ± 5 Ma. Filled circles are from clear co-magmatic zircon cores. Open circle (analysis 7) corresponds to a SHRIMP spot that slightly touches the metamorphic rim and therefore shows some Pb-loss. In (B) analysed spots from both the co-magmatic cores and the metamorphic rims are plotted. Black circles connected with the solid line are from the co-magmatic cores and correspond to those plotted in detail in (A). The gray and white circles are from the metamorphic rims and show different amounts of Pb-loss or are mixed analyses. The gray circles (5 analyses) plot along a mixing line (dashed line) intersecting the concordia at 229 ± 11 Ma, thus indicating a major fluid/metamorphic event at that time (see text). Numbers in italics beside the gray circles correspond to the analyses numbers of table 1. The inset shows a detail of the four analyses considered in the WM age calculation. Error bars are 2σ errors. WM: weighted mean; weighted mean error is given at the 95% confidence level.

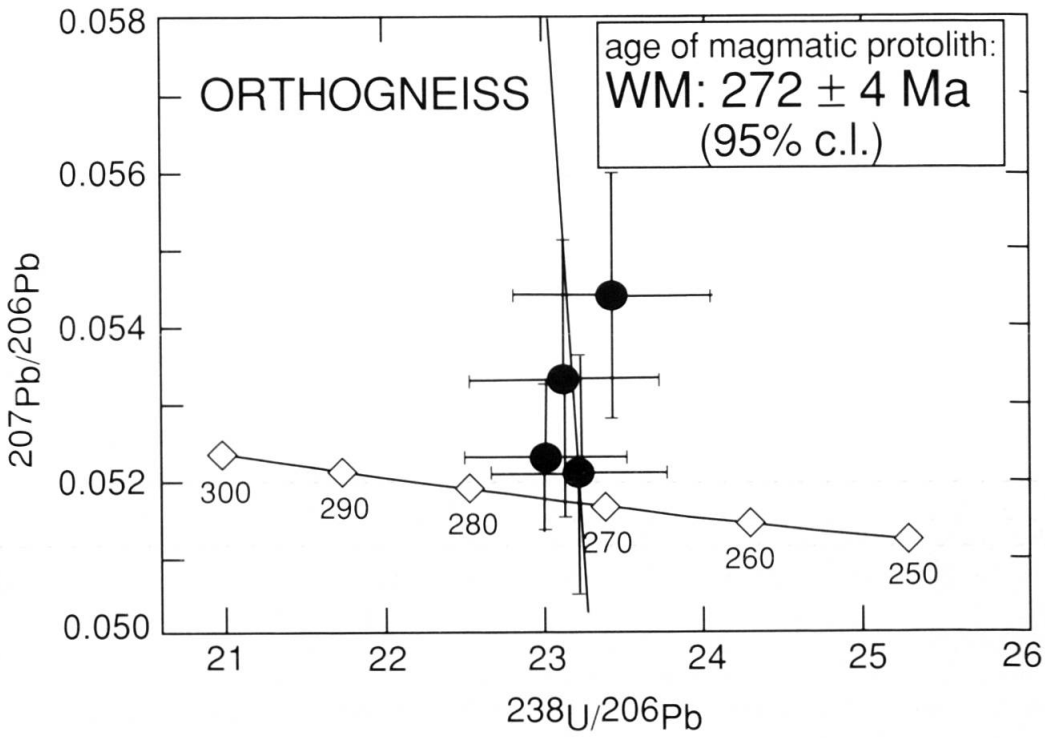

Fig. 6 Tera-Wasserburg diagrams with data of zircons from the orthogneiss of Mattmark. Four analyses from the co-magmatic, oscillatory zoned zircon domains plot along a mixing line intersecting the concordia at 272 ± 4 Ma, which is interpreted as the age of crystallization of the magmatic protolith. Error bars are 2σ errors. WM: weighted mean; weighted mean error is given at the 95% confidence level.

which are usually narrower than the diameter of the SHRIMP spot, as well as their commonly low U content do not allow proper determination of the age(s) of metamorphism. However, the individual $^{206}Pb/^{238}U$ 'ages' scatter between 463 ± 13 Ma and 87 ± 20 Ma (1σ). That is, they range between the magmatic age at 510 ± 5 Ma and a younger metamorphic age. As indicated by post-SHRIMP CL-pictures of the analyzed zircons, the reason for these discordant ages is that the analyzed spot touches part of the older magmatic zircon domain, due to the very small thickness of the rim (e.g. Figs 2B, C). The older magmatic domain lies in some cases just underneath the analyzed metamorphic rim (e.g. Fig. 3A, spot 2, darker CL within the SHRIMP-pit). Given the individual $^{206}Pb/^{238}U$ 'ages' obtained for the metamorphic rims, we can conclude that the youngest metamorphism of these rocks is younger than the lowest 'age' obtained (87 ± 20 Ma), that is Alpine.

An interesting observation is that five of the data points from the metamorphic rims (analyses 11, 12, 15, 17 and 18 of table 1) plot on a mixing line intersecting the concordia at 229 ± 11 Ma (Fig. 5B, gray circles). Omitting analysis 11 (spot 6.1) with 1 ppm U and a very large error (174 ± 58 Ma; 1σ), the remaining 4 analyses yield also a weighted mean age at 229 ± 11 Ma. The fact that these four analyses give the same 'age' within analytical error limits may be interpreted to reflect a major fluid induced metamorphic overprint at that time. More analytical work may resolve this problem. However, it will be difficult to find zircon crystals in these rocks that have metamorphic rims suitable for good SHRIMP analyses (wide enough and with higher U content). As mentioned above (section 3), only when metamorphic temperatures reach those of the upper amphibolite-/granulite-facies, does zircon show well developed wide metamorphic rims derived either by recrystallization of existing magmatic zircon crystals or forming new overgrowths, especially if partial melting occurred. Thus, given this information, precise dating of metamorphism in these rocks is a difficult task.

7.2. LEUCOCRATIC GNEISS (ORTHOGNEISS)

Seven data points were obtained from 4 different grains of zircon from the orthogneiss of Mattmark. Five of them are from co-magmatic, oscillatory zoned core domains, two are from the rims. Four analyses plot along a mixing line with common Pb and $^{238}U/^{206}Pb$ as end members, intersecting the concordia at 272 ± 4 Ma, at the 95% c.l.

(Fig. 6). This is interpreted as the crystallization age of either a granitoid or a rhyolitic protolith. One zircon crystal yielded a 622 ± 9 Ma old core, which is interpreted as inherited. The rim of this inherited zircon grain yielded an 'age' of 351 ± 4 Ma (1σ). Since concordance cannot be demonstrated with only one spot analysis, the 351 ± 4 Ma 'age' is interpreted as resulting most likely from partial Pb-loss due to a later metamorphic event. Again, metamorphic rims were difficult to analyse, because they are very thin (usually <10 μm, smaller than the diameter of the SHRIMP-spot). One spot located in a broader part of the rim yielded a $^{206}Pb/^{238}U$ age of 246 ± 4 Ma (1σ), which indicates Pb-loss during a younger metamorphic event. Although the age of metamorphism is not resolvable at this stage, it is very likely that it is younger than the 246 ± 4 Ma 'age', most probably Alpine (Tertiary). For the same reasons described above for the amphibolitized eclogite of Andolla, precise dating of metamorphism is difficult also for the orthogneiss of Mattmark, due to the size of the metamorphic rims, which are not wide enough to be dated by even a 10 μm SHRIMP spot. The relatively low metamorphic grade of this rock, as well as the apparent presence of low amounts of fluids are probably responsible for poor development of metamorphic rims.

8. Geodynamic implications

Our SHRIMP results exclude an origin as Piemont-Ligurian (Middle/Upper Jurassic) or Valais (Upper Jurassic/Lower Cretaceous) oceanic crust for the precursor of the amphibolitized eclogite in Andolla. An origin from a Mesozoic dyke is also excluded for this locality. Instead, the age data indicate that the protolith of the amphibolitized eclogite was a gabbro that crystallized in Cambrian times (510 ± 5 Ma) and was affected very probably at least by one metamorphic event in Alpine times (after 87 ± 20 Ma). As to the metacarbonates in which the basic boudin is embedded, we still assume – for lithological reasons – that these are Mesozoic in age (see also KELLER and SCHMID, 2001). The occurrence of the Paleozoic mafic boudin of Andolla within Mesozoic metacarbonates can only be explained, in our view, by severe Alpine deformation. Even if these metacarbonates were at one time the original sedimentary cover of the Monte Rosa nappe, they are now part of an Alpine mélange and/or "Schuppenzone". The assumption of KELLER and SCHMID that the locality of Andolla with the dated amphibolitized eclogite boudin belongs to the Monte Rosa sedimentary cover implies a Mesozoic or younger age for the protolith of this eclogite, which is in contradiction with the Cambrian age obtained in the framework of this paper. For this reason, we do not follow KELLER and SCHMID (2001) in assigning this outcrop to the cover of the Monte Rosa nappe, but include it in the Furgg zone. The Paleozoic age of the metagabbro boudin of Andolla, which is tectonically intermingled with likely Mesozoic carbonates, probably indicates, in our view, that the Monte Rosa nappe has no preserved autochthonous Mesozoic sediment cover. Regarding the original paleogeographic position of the metacarbonates, we cannot exclude that they may once have belonged to the cover of the Monte Rosa nappe.

It is worth mentioning that one SHRIMP analysis on the co-magmatic domain of a zircon from the quartz vein located between an eclogite boudin and its country rock at Alpe Campolamana, in a locality that is assigned to the Furgg zone by all previous authors (sample AND3; analyses 8 of table 1), yielded an 'age' of 496 ± 5 Ma. Although the analyzed spot slightly touches a bright CL zone around a crack, thus indicating a slightly mixed analysis of the igneous domain with a domain affected by metamorphism, it is within analytical error limit (2σ) identical to the Cambrian age of 510 ± 5 Ma obtained from the amphibolitized eclogite of Andolla. The identical morphology and CL features of the zircons from this sample (AND3) with those of the eclogite boudin of Andolla (AND1) strongly support the interpretation that they derive from the neighboring amphibolitized eclogite boudin (see above, section 6) thus indicating another locality, besides Andolla, with metabasic rocks of Cambrian protolith age. Therefore, pre-Hercynian crustal components make up at least part of the Furgg zone.

Cambro-Ordovician basic magmatism displaying different geochemical characteristics, i.e. oceanic and active margin settings, is well known from e.g. Cima di Gagnone at 528 ± 6 Ma and Biasca at 521 ± 8 Ma (both in Central Alps; GEBAUER, 1994) or from older orthogneiss of the Silvretta nappe at 525 ± 5 Ma (Eastern Alps; MÜLLER et al., 1995; SCHALTEGGER et al., 1997). Also, an ophiolitic sequence from Chamrousse (Western Alps) was dated at 496 ± 6 Ma (MÉNOT et al., 1988), while coeval granitoid rocks are also reported (see also GEBAUER, 1993 and SCHALTEGGER and GEBAUER, 1999 for a geochronological review of the Central, Western and Southern Alps; THÖNI, 1999 for the Eastern Alps and O'BRIEN et al., 1990; ROHRMÜLLER et al., 1997 for the non-Alpine part of the European Variscides). Although the basic boudin dated in this study yielded a Cambrian age, it is not excluded that other mafic

rocks of the Furgg zone may still be Mesozoic. Indeed, the basic sill within Triassic sediments described by JABOYEDOFF et al. (1996, their figures 5 and 6) is a convincing example of a Mesozoic intrusion.

Interestingly, a Triassic event at ca. 229 ± 11 Ma seems to have affected the amphibolitized eclogite of Andolla. Triassic ages are known from many other geotectonic units of the Alps (e.g. the Ivrea zone, VAVRA et al., 1996; the Sesia zone, RUBATTO and GEBAUER, 2000, or the UHP-rocks of Dora Maira massif, GEBAUER et al., 1997). They have been interpreted to record multi-episodic, rift-related influx of fluids accompanied by local metasomatism and/or deformation (see e.g. SCHALTEGGER et al., 1995; GEBAUER et al., 1997).

Regarding the orthogneiss at Mattmark, it derived from a granitoid or an acid volcanic rock. The Permian age of crystallization obtained for the protolith (272 ± 4 Ma) is in good agreement with recent ages reported for the crystallization of granites of the Monte Rosa massif (U–Pb SHRIMP data on zircon and monazite: 270 ± 4 Ma and 268 ± 4 Ma, respectively; LANGE et al., 2000; combined chemical Th–U–Pb dating of monazite by electron microprobe, XRF-microprobe and isotopic laser ablation PIMMS analysis: ca. 270 Ma; ENGI et al., 2001), as well as for many granitoids all over the Alps and the European Variscides. The SHRIMP ages obtained in the present work for the orthogneiss at Mattmark suggest that it may represent Monte Rosa granite incorporated in the Furgg zone. Additionally, our first data from a kyanite-talc schist (sample MAT5) within a shear zone of the Monte Rosa basement, (see above, section 2), also yielded ages of 274 ± 3 Ma and 276 ± 3 Ma (1σ; analyses 24, 25 of table 1) from probably magmatic domains. These two 'ages' can be considered as additional indication of magmatism at that time. As already mentioned, sample MAT5 is located at the contact between deformed Monte Rosa granite and pre-granitic paragneiss (WEBER 2001). The deformed granite is probably the protolith of this kyanite-talc schist.

The Cambrian age of the protolith of the eclogite boudin in Andolla, as well as the Permian protolith age of the orthogneiss at Mattmark contradict the previous interpretation of JABOYEDOFF et al. (1996) and STECK et al. (1999) that the "middle" and "upper" Furgg zone (to which the dated rocks are attributed) represents a Triassic to Jurassic or even Cretaceous sedimentary cover series crosscut by mafic dykes and associated with syngenetic mafic volcanic rocks, both of which were later boudinaged. Our new SHRIMP age data are in accordance with the suggestion of MILNES et al. (1981) and FROITZHEIM (2001) that the Furgg zone is a mélange of continental basement, Permo-Mesozoic sediments, and Mesozoic ophiolites. It may be that this does not apply for the whole Furgg zone but at least for its northern part, along the northern rim of Monte Rosa nappe. The 496 ± 5 Ma age attributed to the protolith of the amphibolitized eclogite boudin in the area Alpe Campolamana (sample AND3; see above) would support the mélange interpretation for a part of the Furgg zone larger than just the Andolla area. The mélange scenario indicates tectonic mixing of heterogeneous rock constituents in the Furgg zone, e.g. a Cambrian metabasite boudin enclosed in a (for lithological reasons very probably) Triassic metasediment. On the other hand, the presence of Mesozoic ophiolites in the Furgg zone (of Piemont-Ligurian and/or Valaisan origin) has not yet been demonstrated radiometrically. DAL PIAZ (1966) described a series of gneiss, schist, marble, quarzite and amphibolite along the southern border of the Monte Rosa nappe, which is lithologically very similar to the Furgg zone, and interpreted this unit as an "old" (Hercynian) basement. Such an interpretation would be in accordance with our results (if the protolith of the leucocratic gneiss was plutonic, not volcanic), although we think that the strong lithological similarities of some Furgg zone rocks with Triassic sediments (e.g. the metacarbonates enclosing the amphibolitized eclogite of Andolla) argue against an entirely Hercynian nature.

9. Conclusions

The present study leads to the following conclusions and implications:

1. The amphibolitized eclogite of Andolla shows extensive amphibolite-facies overprint marked mainly by the wide development of sodic augite-albite symplectites and alteration to green amphibole. Minimum pressures of ca. 11 kbar are inferred for the HP stage, based on the jadeite content of the analyzed omphacite. For the amphibolite-facies overprint, temperatures of ca. 600 °C result from the garnet-amphibole geothermometer. For the Mattmark orthogneiss, application of the garnet-phengite geothermometer yields metamorphic temperatures between 350° and 510 °C. Based on the Si content of phengite, pressures of ca. 9–11 kbar and 7–8 kbar result for phengite core and rim compositions, respectively. Under these metamorphic conditions, and apparent presence of low amounts of fluids, the zircons of both rock types were only slightly affected during metamorphism, which resulted in the devel-

opment of very thin rims (< ca. 10 μm), as shown in CL-pictures of zircons.

2. The uniform shape, size, CL-patterns (oscillatory zoning with more or less widely spaced domains) and consistent ages from the core domains (magmatic) of the zircons from the amphibolitized eclogite point to a gabbroic protolith. This is supported by the presence of chromite relics in the rock. The size, morphology and oscillatory zoning pattern of the zircons from the Mattmark gneiss, combined with the consistent ages from the core domains, confirm an igneous protolith for this rock.

3. Crystallization of the gabbroic protolith of the Andolla eclogite occurred 510 ± 5 Ma ago. Metamorphism of this rock was Alpine (Tertiary) and took place after 87 ± 20 Ma (the lowest 'age' obtained from the rims). A Triassic fluid/metamorphic event at ca. 229 ± 11 Ma seems to have also affected this rock. The protolith of the Mattmark orthogneiss crystallized 272 ± 4 Ma ago; metamorphism took place most probably in Alpine times (after 246 ± 4 Ma; youngest rim 'age').

4. The Furgg zone is heterogeneous. This study documents the presence of Cambrian basic rocks and Permian granitoids. In addition, based on lithological comparisons (BEARTH, 1953; JABOYEDOFF, 1996; KELLER and SCHMID, 2001) also Permo-Triassic sediments and Mesozoic ophiolites are very probably included, although their presence has not been proven radiometrically.

5. The comparable series on the southern side of the Monte Rosa massif, attributed to the "Furgg zone s.l." by DAL PIAZ (1966) and interpreted as pre-granitic basement with dykes of the Monte Rosa granite, may be equivalent to the rocks that we dated. However, in the Furgg zone (s.s.), along the northern border of the Monte Rosa nappe, these rocks are intercalated with Permo-Triassic sediments and with ophiolites, which is not the case for the series on the southern side.

6. The interpretation of the Furgg zone (at least its northern part along the northern rim of the Monte Rosa nappe) as 'Schuppenzone' (BEARTH, 1953) or tectonic mélange (MILNES et al., 1981; KRAMER 2000; FROITZHEIM, 2001) is compatible with our results. Additional radiometric data would certainly shed more light on the problem of the nature and extent of the Furgg zone.

Acknowledgements

We acknowledge the help of R.A. Stern and M. Hamilton (GSA, Ottawa) during various stages of SHRIMP work. Thanks are due also to P. Meyer (Heidelberg) for his assistance during microprobe work. L. Keller (Basel) found and mapped the Andolla outcrop of the dated amphibolitized eclogite. A. Weber (Bonn) contributed unpublished results of mapping in the Mattmark area. Discussions with the participants of the Monte Rosa field trip 2001, and constructive reviews by M. Engi, B. Seth and Th. Nägler (Bern) are greatly appreciated. This work was supported by a grant of the Swiss National Science Foundation (20-52662.99).

References

BEARTH, P. (1952): Geologie und Petrographie des Monte Rosa. Beitr. Geol. Karte Schweiz (Neue Folge) 96, 1–94.

BEARTH, P. (1953): Geologischer Atlas der Schweiz, 1: 25'000, Blatt 535 Zermatt. Schweiz. Geol. Komm.

CUMMING, G.L. and RICHARDS, G.R. (1975): Ore lead isotope ratios in a continuously changing Earth. Earth Planet. Sci. Lett. 28, 155–171.

DAL PIAZ, G.V. (1966): Gneiss ghiandoni, marmi ed anfiboliti antiche del ricoprimento Monte Rosa nell'alta Valle d'Ayas. Bolletino della Societá Geologica Italiana 85, 103–132.

DAL PIAZ, G.V. (2001): Geology of the Monte Rosa massif: historical review and personal comments. Schweiz. Mineral. Petrogr. Mitt. 81, 275–303.

ENGI, M., SCHERRER, N.C. and BURRI, TH. (2001): Metamorphic evolution of pelitic rocks of the Monte Rosa nappe: Constraints from petrology and single grain monazite age data. Schweiz. Mineral. Petrogr. Mitt. 81, 305–328.

ESCHER, A., HUNZIKER, J.C., MARTHALER, M., MASSON, H., SARTORI, M. and STECK, A. (1997): Geologic framework and structural evolution of the western Swiss-Italian Alps. In: PFIFFNER, O.A., LEHNER, P., HEITZMANN, P., MÜLLER, S. and STECK, A. (eds): Deep Structure of the Swiss Alps – Results from NRP 20: Basel, Switzerland, Birkhäuser, p. 205–221.

FROITZHEIM, N. (2001): Origin of the Monte Rosa nappe in the Pennine Alps – A new working hypothesis. Bull. Geol. Soc. Am. 113, 604–614.

GASPARIK, T. and LINDSLEY, D.H. (1981): Phase equilibria at high pressures of pyroxenes containing monovalent and trivalent ions. In: PREWITT, C.T. (ed.): MSA Reviews in Mineralogy 7, Pyroxenes, 309–339.

GEBAUER, D. (1993): The Pre-Alpine evolution of the continental crust of the Central Alps – an overview. In: VON RAUMER, J.F. and NEUBAUER, F. (eds): Pre-Mesozoic Geology in the Alps. Springer Verlag, 93–117.

GEBAUER, D. (1994): A P-T-t path for some high-pressure ultramafic/mafic rock associations and their felsic country rocks based on SHRIMP-dating of magmatic and metamorphic zircon domains. Example: Central Swiss Alps. Extended abstract, 16th general meeting of IMA, Pisa, Italy, Sept. 4–9, 139–140.

GEBAUER, D. (1996): A P-T-t path for a (ultra?-) high-pressure ultramafic/mafic rock associations and their felsic country-rocks based on SHRIMP-dating of magmatic and metamorphic zircon domains. Example: Alpe Arami (Central Swiss Alps). In: BASU, A. and HART, S. (eds): Earth Processes: Reading the Isotopic Code; Geophysical Monograph Series 95, 307–329.

GEBAUER, D. (1999): Alpine geochronology of the Central and Western Alps: new constraints for a complex geodynamic evolution. Schweiz. Mineral. Petrogr. Mitt. 79, 191–208.

GEBAUER, D., SCHERTL, H.-P., BRIX, M. and SCHREYER, W. (1997): 35 Ma old ultrahigh-pressure metamorphism and evidence for very rapid exhumation in the Dora-Maira Massif, Western Alps. In: SCHREYER, W. and STÖCKHERT, B. (eds): HP-metamorphism in nature and experiment. International lithosphere programme, contribution 327. Special Issue, Lithos 41, 5–24.

GRAHAM, C.M. and POWELL, R. (1984): A garnet-hornblende geothermometer: calibration, testing and application to the Pelona Schist, Southern California. J. Metamorphic Geol. 2, 13–21.

GREEN, T.H. and HELLMAN, P.L. (1982): Fe–Mg partitioning between coexisting garnet and phengite at high pressure, and comments on a garnet-phengite geothermometer. Lithos 15, 253–266.

GÜLLER, A. (1947): Zur Geologie der südlichen Mischabel- und der Monte Rosa-Gruppe. Eclogae geol. Helv. 40, 39–161.

HYNES, A. and FOREST, R.C. (1988): Empirical garnet-muscovite geothermometry in low-grade metapelites, Selwyn Range (Canadian Rockies). J. Metamorphic Geol. 6, 297–309.

JABOYEDOFF, M., BÉGLÉ, P. and LOBRINUS, S. (1996): Stratigraphie et évolution structurale de la zone de Furgg, au front de la nappe du Mont-Rose. Bulletin de la Société Vaudoise des Sciences Naturelles 84, 191–210.

KELLER, L.M. (2000): Kinematik der duktilen Scherung an der Front der Monte Rosa Decke. Unpubl. Diploma Thesis, Basel University.

KELLER, L.M. and SCHMID, S.M. (2001): On the kinematics of shearing near the top of the Monte Rosa nappe and the nature of the Furgg zone in Val Loranco (Antrona valley, N. Italy): tectonometamorphic and paleogeographical consequences. Schweiz. Mineral. Petrogr. Mitt. 81, 347–367.

KRAMER, J. (2000): The Penninic units in the Monte Rosa region: new structural and metamorphic evidence for the provenance of the continental nappes. 17th Swiss Tectonics Studies Group Meeting, Zürich, 31. March–1. April, 2000, Abstract Volume p. 50.

KROGH, E.J. and RAHEIM, A. (1978): Temperature and pressure dependence of Fe–Mg partitioning between garnet and phengite, with particular reference to eclogites. Contrib. Mineral. Petrol. 66, 75–80.

LANGE, S., NASDALA, L., POLLER, U., BAUMGARTNER, L. and TODT, W. (2000): Crystallization age and metamorphism of the Monte Rosa granite, Western Alps. 17th Swiss Tectonics Studies Group Meeting, Zürich, 31. March–1. April, 2000, Abstract Volume, p. 51.

MASSONNE, H.J. and SCHREYER, W. (1987): Phengite geobarometry based on the limiting assemblage with K-feldspar, phlogopite and quartz. Contrib. Mineral. Petrol. 96, 212–224.

MÉNOT, R.P., PEUCAT, J.J., SCARENZI, D. and PIBOULE, M. (1988): 496 Ma age of plagiogranites in the Chamrousse ophiolitic complex (external crystalline massifs in the French Alps): evidence of a Lower Paleozoic oceanization. Earth Planet. Sci. Lett. 88, 82–92.

MILNES, A.G., GRELLER, M. and MÜLLER, R. (1981): Sequence and style of major post-nappe structures, Simplon-Pennine Alps. J. Struct. Geol. 3, 411–420.

MÜLLER, B., KLÖTZLI, U. and FLISCH, M. (1995): U–Pb and Pb–Pb dating of the older orthogneiss suite in the Silvretta nappe, Eastern Alps: Cadomian magmatism in the upper Austroalpine realm. Geol. Rundschau 84, 457–465.

O'BRIEN, P.J., CARSWELL, D.A. and GEBAUER, D. (1990): Eclogite formation and distribution in the Central European Variscides. In: CARSWELL, D.A. (ed.): Eclogite Facies Rocks. Blackie, New York, 204–220.

PACES, J.B. and MILLER, J.D. (1993). Precise U–Pb ages of Duluth Complex and related mafic intrusions, northeastern Minnesota: Geochronological insights to physical, petrogenetic, paleomagnetic, and tectonomagmatic process associated with the 1.1 Ga Midcontinent Rift System. J. Geophys. Res. 98, 13997–14013.

ROHRMÜLLER, J., MIELKE, H. and GEBAUER, D. (1997): Gesteinsfolge des Grundgebirges südlich der Donau und im Molasseuntergrund. In: Erläuterungen zur Geologischen Karte von Bayern 1 : 500 000. Verlag: Bayerisches Geologisches Landesamt, 16–50.

RUBATTO, D. and GEBAUER, D. (2000): Use of Cathodoluminescence for U–Pb zircon dating by ion microprobe: some examples from the Western Alps. In: PAGEL, M., BARBIN, V., BLANC, P. and OHNENSTETTER, D. (eds): Cathodoluminescence in Geosciences. Springer Verlag, 373–400.

SCHALTEGGER, U. and GEBAUER, D. (1999): Pre-Alpine Geochronology of the Central, Western and Southern Alps. Schweiz. Mineral. Petrogr. Mitt. 79, 79–87.

SCHALTEGGER, U., NÄGLER, TH.N., CORFU, F., MAGGETTI, M., GALETTI, G. and STOSCH, H.G. (1997): A Cambrian island arc in the Silvretta nappe: constraints from geochemistry and geochronology. Schweiz. Mineral. Petrogr. Mitt. 77, 337–350.

SCHALTEGGER, U., ZWINGMANN, H., CLAUER, N., LARQUÉ, P. and STILLE, P. (1995): K–Ar dating of a Mesozoic hydrothermal activity in Carboniferous to Triassic clay minerals of northern Switzerland. Schweiz. Mineral. Petrogr. Mitt. 75, 162–176.

STECK, A., BIGIOGGERO, B., DAL PIAZ, G.V., ESCHER, A., MARTINOTTI, G. and MASSON, H. (1999): Carte tectonique des Alpes de Suisse occidentale 1:100000, Service hydrologique et géologique national, Bern.

THÖNI, M. (1999): A review of geochronological data from the Eastern Alps. Schweiz. Mineral. Petrogr. Mitt. 79, 209–230.

VAVRA, G.F., GEBAUER, D., SCHMID, R. and COMPSTON, W. (1996): Multiple zircon growth during polyphase Late Carboniferous to Triassic metamorphism in granulites of the Ivrea Zone (Southern Alps): an ion microprobe (SHRIMP) study. Contrib. Mineral. Petrol. 122, 337–358.

WEBER, A. (2001): Zur strukturellen und metamorphen Entwicklung der Furgg-Zone und angrenzender Einheiten im südlichen Saastal, Wallis, Schweiz. Unpubl. diploma thesis, Bonn University.

WETZEL, R. (1972): Zur Petrographie und Mineralogie der Furgg-Zone (Monte Rosa-Decke). Schweiz. Mineral. Petrogr. Mitt. 52, 161–236.

WILLIAMS, I.S. (1998): U–Th–Pb Geochronology by Ion Microprobe. In: MCKIBBEN, M.A., SHANKS III, W.C. and RIDLEY, W.I. (eds): Applications of microanalytical techniques to understanding mineralizing processes. Reviews in Economic Geology 7, 1–35.

Manuscript received July 11, 2001; revision accepted November 6, 2001.